GEOPHYSICAL AND GEOSTATISTICAL RESERVE ESTIMATES OF MIGMATITE-GNEISS DEPOSITS FROM PARTS OF SOUTHWESTERN NIGERIA

ADEMILA, OMOWUMI

ABSTRACT

The plan for durable rock base road construction and other civil engineering works necessitated this study to establish the thickness and quantify migmatite-gneiss deposits. This intends to facilitate its exploitation and proffer specific details for diverse applications. Comprehensive geological field mapping, laboratory density measurements and geoelectrical resistivity were employed for the resource quantification. The extent of migmatite-gneiss deposits and its contacts with other rock types were identified. Seventeen (17) fresh migmatite-gneiss rock samples collected from different rock outcrops were taken to the laboratory for measurement of their density. Schlumberger vertical electrical sounding (VES) technique with a total of forty-two sounding stations were employed across the area with electrode spread (AB/2) ranging 1 - 200 m. The average density of the deposits is 2.70 ± 0.10 g/cm^3. Three to five geologic layers characterized the area subsurface sequence. Thick fractured rock layer across the area would facilitate the exploitation of the deposits as construction aggregates. Basement topographical highs at northeastern, northwestern and southeastern parts serve as the best zones viable for mining. The basement resistivity (> 3000 Ωm), resistivity contrast, reflection coefficient values and high transverse layer resistivity (ρ_T) (> 500 Ωm) corroborate the freshness of the deposits. The average thickness of the deposit is 29.3 m, though, thicker at northeastern and northwestern parts of the area where the deposit is fresh and less weathered. The study area occupies a total area of 71,300,000 m^2 with volume of the deposits calculated as 2,089,090,000 m^3. Distantly-spaced data points of the variogram reveal high degree of variability with respect to locations. The estimated migmatite-gneiss resource tonnage of 5,640,543,000 tonnes shows prospects for sustainable large scale mining as construction aggregates and diverse applications of economic purposes using open pit coupled with underground mining for deeper sections of the migmatite-gneiss deposit.

KEYWORDS: Migmatite-gneiss deposits, reserve estimate, variogram, density measurement, geoelectric parameters

INTRODUCTION

Migmatite, a mixed rock formed by anatexis, from partial melting which occurs when a pre-existing rock is exposed to high temperature and pressure. Its distinct characteristics from microscopic to macroscopic scale confirm its composite nature of metamorphic and igneous rocks (Sawyer, 2008). Alternating layers of rich mafic mineral darker layers (melanosomes) and lighter layers of quartzofeldspathic minerals (leucosomes) make up the migmatite rock. The mafic mineral dark layers consist of dark-coloured minerals like amphibole, biotite and show attributes of metamorphic rocks (amphibolite or gneiss), while the lighter layers consist of light-coloured minerals (feldspar, quartz and muscovite) and they are granitic in texture (Pawley et al., 2015). The light-coloured layers from partial melting have igneous features, while the dark-coloured layers have undergone metamorphism.

Migmatites are beautiful, amazing hybrid metamorphic and igneous rocks with undulating black and white shades of appearance extensively used as aggregates and building stones in civil engineering works. The rare features of migmatites make it useful in cement manufacture, as dimension stone and road aggregate. It can also be polished as ornament for interior and exterior decoration. Gneiss is a widely spread metamorphic rock formed under high temperature and high pressure conditions. Migmatites are similar to gneisses; they are relative rock types with alternating light and dark layers. The foliated metamorphic rock (gneiss) forms through high-grade, regional metamorphism are recognized by lenses and bands of different mineralogy. Gneiss is distinguished by the banded appearance and texture with the light coloured bands formed through recrystallization. The alternating mineral layers referred to as gneissic banding characterized the rock with the recrystallized mineral

Ademila, Omowumi, Department of Earth Sciences, Adekunle Ajasin University, Akungba-Akoko, Nigeria

grains under high temperature and pressure (Marshak, 2013). The gneissic banding, which is a distinct type of foliation exhibits by gneiss rocks differentiate it from other foliated rocks. Mineralogical composition of gneiss includes quartz, mica, chlorite, feldspar and other clay minerals. Larger crystals of topaz, garnet and beryl minerals are also contained in some gneiss rock matrix. Some minerals also imbedded in gneiss like garnet, sillimanite, andalusite, staurolite, biotite, kyanite and cordierite, are used in naming the rocks such as biotite gneiss, granite gneiss and garnet gneiss (Robertson, 1999). Gneiss finds useful applications in civil engineering construction works; as crushed stone/construction aggregate in road construction for asphalt pavement, landscaping works and building site preparation because of its resistant to fracture. The durability characteristics of gneiss makes it suitable as dimension stone and can be sheared and cut into slabs and blocks for diverse paving, building and curbing works. Polished gneiss can be used as architectural stone and glittery look of most of the gneisses makes it applicable in window sills, flooring, stair treads, gravestones, facing stones and countertops. Low water absorption and strength characteristics of the rock make it sound and suitable as civil engineering construction rock aggregates. The rock type also possesses the required quality standard for bituminous mixes and construction aggregates in highway pavements and foundations (Ademila, 2019). Electrical resistivity techniques have been gainfully employed in engineering site to investigate and image the subsurface disposition by measuring electrical properties of geomaterials. This in turn has been used in unraveling the stratigraphic sequence of geomaterials, subsoil competence, overburden thickness, nature and distribution of geologic structures and depth to basement (Ademila et al., 2020; Ademila, 2021; Ademila, 2022). These effective non-invasive and non-destructive geophysical tools for subsurface investigation also offer information on quantitative estimates of geologic deposits, geomorphology and tectonic activity of areas (Bufford et al., 2012; Ademila, 2022). Evaluation of parameters of geological significance in mineral exploration; thickness, grade, reserve/resource estimation, approximate accumulation and appropriate accuracy evaluation are essential tasks of a geoscientist coupled with geostatistical analysis for accurate resource quantification (Kokesz, 2006). The plan for durable road construction and rehabilitation of failed major roads to rock base in order to bear heavy traffic load necessitated the estimation of extensive migmatite-gneiss deposits in the area. The findings would be beneficial to the government, residents and general populace as reserve estimate of the deposit would boost its future utilization as construction aggregates for road pavement, building site preparation, landscaping works and series of applications based on its unique and attractive features.

SURVEY AREA (location and geological setting)

The survey area is in the northern parts of Ondo State, Nigeria and lies between Longitudes 5° 30' E and 5° 50' E and Latitudes 7° 10' N and 7° 35' N (Fig. 1). It is within the rain forest zone of southwestern Nigeria, distinguished by rainy and dry seasons, having an average rainfall above 1,500 mm per annum. It has broad vegetation with 27°C and above 70% temperature and relative humidity respectively. The survey area covers the towns of Oba, Ayegunle, Iwaro-Oka, Eti-Oro, Akungba, Ikare, part of Owo, villages of Eti-Ose and Ago-Igbira, Southwestern Nigeria. The area is characterized with gently undulating basement relief (topography) from low lands to hilly terrain and surface elevation of over 345 m. Three different rock units make up the Precambrian Basement Complex rocks of Nigeria, which are the migmatite-gneiss-quartzite complex, schist belts and older granites. The survey area situates in basement complex geological setting of southwestern Nigeria, underlain by migmatite-gneiss-quartzite complex. Distribution of various rock types and their contacts were identified and delineated through detailed geological mapping of the area. It consists of migmatite gneiss, quartzite, charnockite, grey gneiss, granite gneiss and older granite (Rahaman, 1989) with predominantly massive and extensive migmatite gneiss (Fig. 1) of quartzite patches and pegmatites intrusion. The composition of migmatite-gneiss is granitic with varying aplitic – granitic – pegmatitic texture and contorted foliations (Hamblin and Howard, 2005). Quartzite-schist, granodiorite, charnockite and fine to medium grained biotite granite form the minor rock units of the area. The extensive migmatite gneiss exists as ridges and hills with series of dykes, quartz veins, pegmatitic veins and quartzo-feldspathic intrusion. The migmatite gneiss of the survey area is categorized into three components; grey gneiss, felsic component and granite gneiss (Rahaman and Ocan, 1978). The light and dark grey gneisses are foliated with coloured thin and thick bands of diverse mineralogy. The common linear and planar rock fabrics of medium grained grey gneiss of persistent banding are observed with alternating light and dark layers. It also occurs as boulders, low lying outcrops and hills. The basement rocks trending N-S direction are characterized by geologic structures; fracture, folds, joints, faults, xenoliths. Textural analysis on the field reveals different gneiss types but the medium grained banded gneiss having thin and thick bands is prominent with foliation dipping in the range 48° to 76°. The estimate of migmatite gneiss of interest in this study area which occurs as extensive hills would provide specific details in quarrying for diverse applications. The following Rivers; Ogbese, Alatan, Agbo, Ose, Awara, Ako, Isakare and their tributaries constitute the drainage network system of the area in a dendritic form/pattern (Ademila, 2019), which comparatively implies uniform weathering resistance of subsurface rocks.
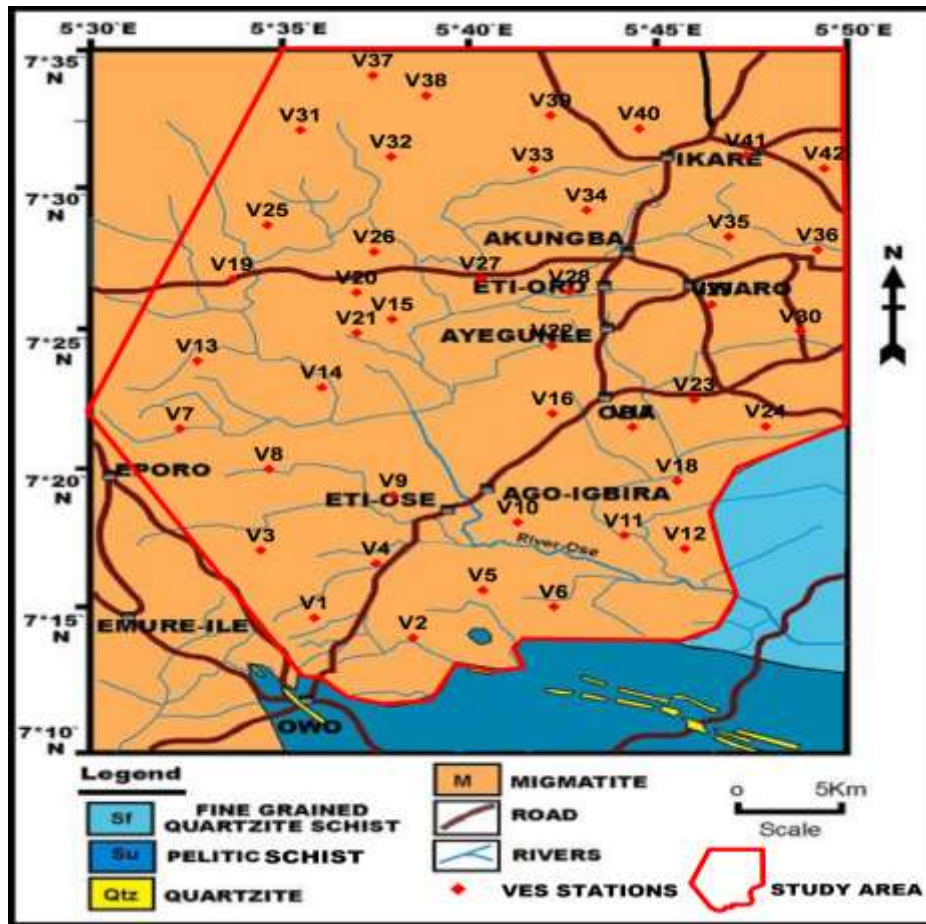
Figure 1: Geological map of the survey area showing the geophysical field layout.

MATERIALS AND METHODS OF STUDY

Geological and geophysical mapping

Comprehensive geological field mapping was carried out to determine the different rock types in the area with recorded coordinates using a global positioning system (GPS). The extent of migmatite gneiss and its contacts with other rock formations were considered. This resulted into the production of detailed geological map of the area. During this geological mapping, geophysical traverses were established and sounding stations were set up from which the geophysical data were acquired (Fig. 1). Geoelectrical resistivity and laboratory density measurements were employed in this study. Geoelectrical resistivity method depends on the passage of electrical current into the earth for its response, from which electrical impedance of geomaterial are measured. Measurements of subsurface resistivity are connected with depth variation with respect to the distance/spread between the current electrodes and potential electrodes of the geoelectric survey. The resistivity measurements are subsequently processed and interpreted (quantitatively and qualitatively) in form of subsurface lithologic model. Resistivities of the earth are in the range above nine orders of magnitude (1 – 10^8 Ωm) (Telford et al., 1990). The electrical resistivity investigation employed Schlumberger vertical electrical sounding (VES) technique with a total of forty-two sounding stations occupied across the entire area of study. The VES data were acquired using ABEM SAS 1000 terrameter with the electrode spread (AB/2) ranging 1 - 200 m. This non-invasive technique presents requisite information of subsurface rock properties from

varying electrode separation (Ademila, 2021; Ademila, 2022). VES measurements probe the vertical variation in resistivity distribution of geomaterials at each sounding station with depth. The Schlumberger electrode configuration offers good geologic signal, good visual horizontal layer resolution and quality sensitivity of depth (Ward, 1990). The data acquired were processed by plotting apparent resistivity against AB/2 on bi-log graph. The processed data were thereafter presented as field curves. The data were partially curve matched by using two-layer master curves and appropriate auxiliary charts as the first round investigation (Koefoed, 1979; Zohdy, 1973). This offers the resistivity and thickness of different layers of subsurface geomaterials at every VES station. WinResist software was utilized for the computer iteration of the curve matched data (initial model). This computer data iteration serves as the last stage of the interpretation from which the geoelectric parameters are generated (Vander Velper, 2004). The computer interpretation program input the initial derived geoelectric parameter, consecutively improved on the data until the root mean square error (RMS-error) is reduced to an acceptable level of < 5.0. Geoelectric sections were thereafter constructed from the modeled subsurface parameters.

Sampling and distribution of rock samples

Seventeen (17) fresh rock samples were collected from different rock outcrops of grey gneiss/biotite gneiss (5 samples), granite gneiss (4 samples), migmatite (5 samples) and gneiss; biotite-granite banded gneiss (3 samples) situated across the study area. These rock types were selected for laboratory measurement due to

their widespread and abundance in the area. The rock outcrop at each location was properly examined and described. Then the samples were taken to the laboratory for measurement of their density.

Laboratory density measurement of rock samples

Density is a significant rock attribute used to classify rock type and its geologic structure, its measurement requires correctly determining mass and volume of rock samples, because the ratio of mass to volume gives value of the density. Fresh rock samples were used for the measurement as weathering process alters the mineralogical composition of original rock and changes its density. Archimedes principle was applied to determine the density of the samples. Mass of each sample was accurately measured with an electronic scale balance and recorded in grams. The volume was determined by placing the rock into a graduated cylinder filled with water, ensuring the rock sample is completely covered with water. The exact volume of the water in the graduated cylinder was recorded with the aid of the cylinder scale. After which, the rock sample was placed inside the cylinder and the final volume was recorded. The difference between the final volume and initial volume was calculated as the volume of the rock sample.

The formula involved in the laboratory measurement of the rock samples is stated as:

$\rho = m/v$ (g/cm^3)

where ρ, m and v represent rock density, mass of the rock and rock volume. All the rock samples measured show no pore space, so the values of the rock density determined correspond closely to the original rock grain density with result accuracy of about 1% or in the range ± 0.02 g/cm^3.

Geostatistical analyses have been widely applied to metal and non metal resource analyses to determine spatial variability of ore grade in a deposit, resource quality and reserve assessment (Heriawan and Koike, 2008). Geostatistical analysis of the data acquired with respect to particular rock types distributed across the area also enhances the resource quantification. It predicts the variation of properties of geological systems over the areas from observed values. In this study, geostatistical analysis was used to estimate the spatial correlations of the data acquired to predict accuracy of the values based on relationship between location and acquired data.

RESULTS AND DISCUSSION

Summary of the density values of the laboratory measured rock samples are presented in Table 1. Mean rock density values of 2.70, 2.63, 2.72 and 2.77 g/cm^3 were obtained for migmatites, biotite gneisses, granite gneisses and banded gneisses respectively distributed in the area. The crystalline basement rocks generally reflect densities higher than 2.60 g/cm^3, which is an indication of measurement of fresh rock samples with unaltered mineralogy. The density range of migmatite-gneiss in the study area is 2.56 – 2.88 g/cm^3 with an average density of 2.70 ± 0.10 g/cm^3 (Table 1). Subsurface information and disposition of different locations investigated is revealed by resistivity responses of geology/geomaterials of the area. Eight
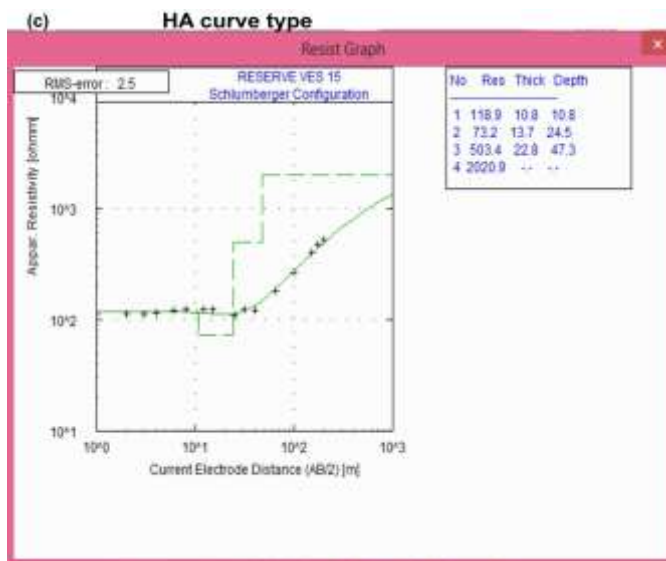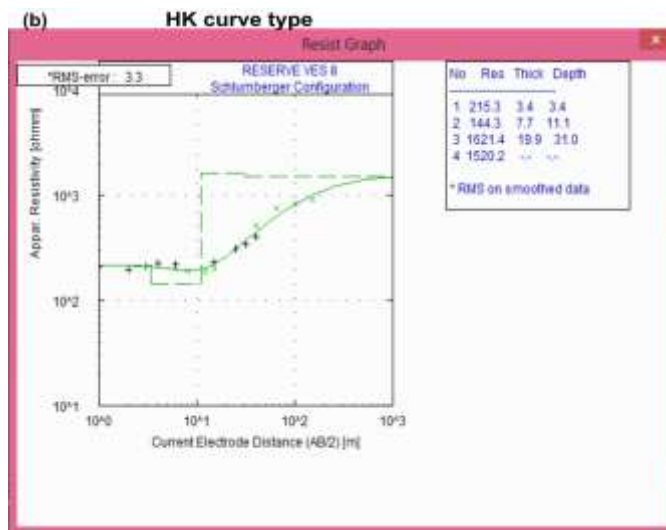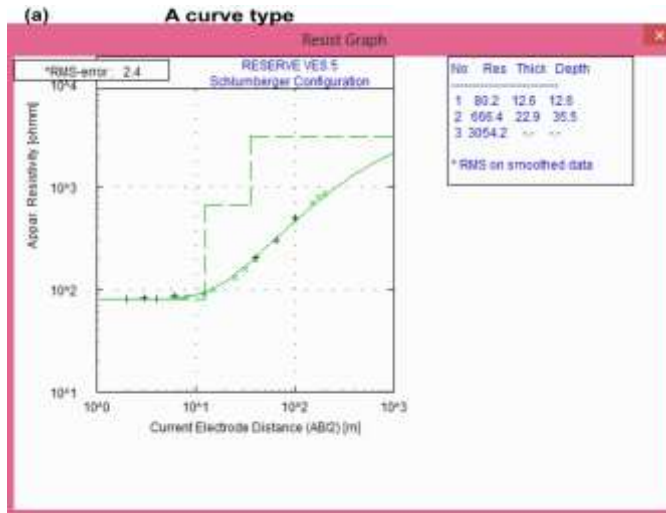
different type curves (A, AA, HA, HK, KH, AKH, HKH and KHK) are obtained from the processed geoelectric field data (Table 2 and Fig. 2). HA is the predominant VES curve type in the study area with 31% occurrence, followed by AA (24%), A (14%), HKH (10%), AKH, KHK (7%), KH (5%) and HK (2%) (Fig. 3). High occurrence of HA followed by AA type curves signify complex geologic setting of the area with high resistive bedrock (host rock). The HA is typical geological representation of low resistive weathered basement beneath resistive topsoil, followed by fractured substratum and high resistive bedrock, while AA is also a 4-layer geologic setting of increasing resistivity response from the topsoil to the fresh basement. Geoelectric sections constructed from the electrical resistivity subsurface (geoelectric) parameters generated from the derived model are presented in Figs. 5 – 11, which shows the geoelectric nature of the distributed geological units in the area with depth. Three to five distinctive subsurface layers representing the geological sequence existing in the area, which include: topsoil characterized by clay/sandy clay/clayey sand and lateritic sand, lateritic layer, weathered basement, partially weathered/fractured substratum and fresh basement. Prospective zones with resistivity response ≥ 1000 Ωm are classified as fresh bedrock/fresh basement rock. The resistivity response of the topmost layer (topsoil) in the range 34 – 524 Ωm suggests clay, sandy clay and clayey sand/laterite with thickness 1.1 – 22.2 m. Different soil composition of the topsoil is responsible for its resistivity variation. Clay and sandy clay constitute the main composition of weathered layer in the area with respective resistivity and thickness range of 38 - 209 Ωm and 3.9 – 41.2 m. Thick lateritic geologic layer (5.3 – 33.2 m) in some locations of the study area having resistivity range 257 - 1615 Ωm are influenced by geology of the basement complex terrain. Prominent fracture system trending the area signify potential subsurface channel for groundwater. Partially weathered/fractured rock layer localized in the area would enhance exploitation of the migmatite-gneiss deposits for diverse applications. This rock layer having resistivity range 273 - 944 Ωm is sufficiently thick (11.1 – 109 m – infinity (∞)) to permit its utilization as aggregates in construction of roads, airfields, buildings, highways and earth dams for sustainable socio-economic development of the area and its environs. Resistivity response of the fresh bedrock in the range 1007 – 36873 Ωm indicates uneven bedrock topography with depth to basement 16.1 – 135.4 m. The variation in resistivity of the geologic rock units is as a result of the varied mineralogy, extent of weathering and diverse structural features of the rocks. The thickness of fractured rock layer and fresh bedrock in the area would make the deposit viable for large-scale economic mining as construction grade stone for industrial/economic purposes considering the positive impact the extractive industries would have on the economy and the society. The geoelectrical characteristics of the subsurface layers have provided insights into the disposition and extent of occurrence of the migmatite gneiss deposits in the area.
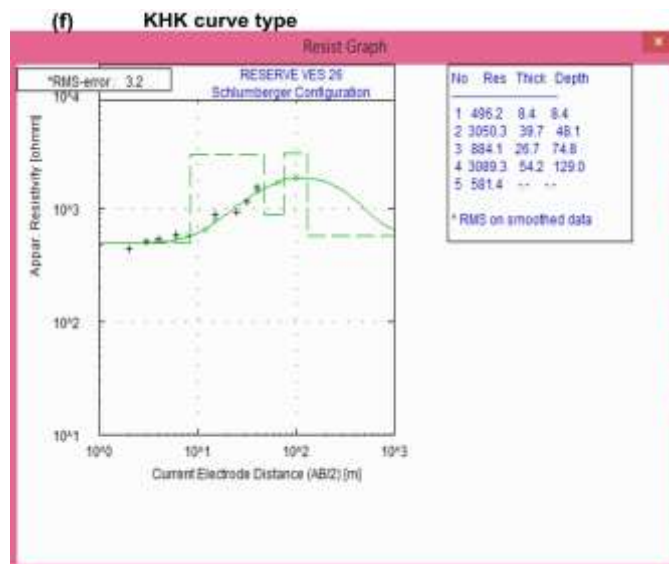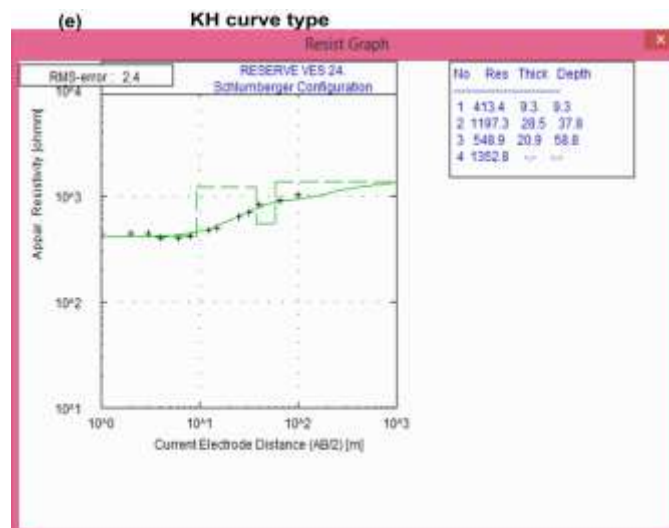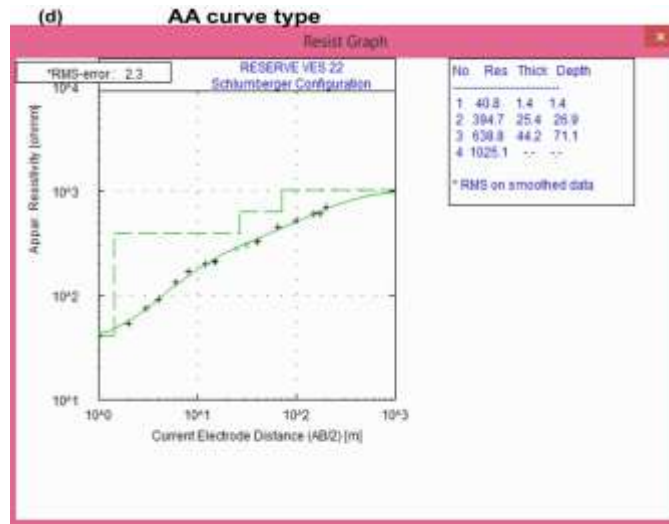
Table 1: Summary of density values of the rock samples

Rock sample No.	Rock type	Rock mass (g)	Rock volume (cm^3)	Rock density (g/cm^3)	Mean (g/cm^3)	Range (g/cm^3)
Mg1	Migmatite	21.17	8.00	2.65	2.70	2.60 – 2.88
Mg2	Migmatite	21.45	8.00	2.68		
Mg3	Migmatite	20.32	7.50	2.71		
Mg4	Migmatite	20.16	7.00	2.88		
Mg5	Migmatite	22.11	8.50	2.60		
Bg1	Biotite gneiss	19.61	7.50	2.61	2.63	2.59 – 2.68
Bg2	Biotite gneiss	21.52	8.30	2.59		
Bg3	Biotite gneiss	22.08	8.50	2.60		
Bg4	Biotite gneiss	20.09	7.50	2.68		
Bg5	Biotite gneiss	21.22	8.00	2.65		
Gg1	Granite gneiss	23.01	9.00	2.56	2.72	2.56 – 2.88
Gg2	Granite gneiss	19.73	7.00	2.82		
Gg3	Granite gneiss	22.31	8.50	2.62		
Gg4	Granite gneiss	20.14	7.00	2.88		
Gn1	Banded gneiss	20.24	7.50	2.70	2.77	2.70 – 2.81
Gn2	Banded gneiss	19.59	7.00	2.80		
Gn3	Banded gneiss	21.07	7.50	2.81		
				Mean = 2.70 g/cm^3 or 2700 kg/m^3 Range = 2.56 – 2.88 S.D. = 0.10		

Table 2: Subsurface geoelectrical parameters of the interpreted VES curves

VES No.	VES Location	Resistivity (Ohm-m)					Thickness (m)				Curve type	Resistivity contrast	R_c	ρ_T (Ωm)
		ρ1	ρ2	ρ3	ρ4	ρ5	h1	h2	h3	h4				
1	Emure-Ile	161	466	1213	3100		3.6	6.9	12.4		AA	2.56	0.44	822.5
2	Emure-Ile	159	390	2068			9.2	16.8			A	5.30	0.68	308.3
3	Owo	97	430	5720			8.3	9.7			A	13.30	0.86	276.5
4	Owo	105	479	97	1106		1.7	8.0	24.9		KH	11.40	0.84	185.7
5	Owo	80	666	3054			12.6	22.9			A	4.59	0.64	458.0
6	Owo	59	553	1995			6.8	22.4			A	3.61	0.57	438.0
7	Eporo	426	164	351	1130		1.6	6.7	22.9		HA	3.22	0.53	314.7
8	Eti-Ose	215	144	1621	1520		3.4	7.7	19.9		HK	0.94	-0.03	1100.0
9	Eti-Ose	100	141	1874	2285		2.4	12.4	26.7		AA	1.22	0.10	1253.6
10	Ago-Igbira	289	48	631	3016		2.2	6.7	16.0		HA	4.78	0.65	443.9
11	Ago-Igbira	89	130	865	2633		4.7	12.2	18.1		AA	3.04	0.51	504.6
12	Ago-Igbira	97	209	944	2578		9.5	13.6	18.4		AA	2.73	0.46	509.2
13	Eporo	77	437	1007	1975		5.5	12.0	26.9		AA	1.96	0.33	737.7
14	Eporo	34	369	1899	7036		5.5	5.3	14.5		AA	3.71	0.58	1173.1
15	Ayegunle-Oka	119	73	503	2021		10.8	13.7	22.8		HA	4.02	0.60	290.8
16	Oba-Akoko	57	404	1556			3.6	14.2			A	3.85	0.59	333.8
17	Oba-Akoko	68	703	1920			5.1	11.1			A	2.73	0.46	503.1
18	Oba-Akoko	181	62	771	1670		1.6	4.0	16.5		HA	2.17	0.37	600.0
19	Ayegunle-Oka	226	82	577	2184		2.5	5.6	14.4		HA	3.79	0.58	414.8
20	Ayegunle-Oka	210	44	630	1926		3.4	11.9	25.3		HA	3.06	0.51	423.1
21	Ayegunle-Oka	179	401	663	1372		5.2	17.4	26.9		AA	2.07	0.35	520.1
22	Ayegunle-Oka	41	395	639	1025		1.4	25.4	44.2		AA	1.60	0.23	539.9
23	Oba-Akoko	490	200	763	3505		1.1	7.6	19.8		HA	4.59	0.64	602.3
24	Oba-Akoko	413	1197	549	1353		9.3	28.5	20.9		KH	2.46	0.42	842.1
25	Eti-Oro	425	1615	836	3939	703	20.2	31.5	15.3	53.3	KHK	0.18	-0.70	2345.8
26	Eti-Oro	496	3050	884	3089	581	8.4	39.7	26.7	54.2	KHK	0.19	-0.68	2451.8
27	Eti-Oro	451	4233	848	4782	660	19.7	38.2	17.5	59.9	KHK	0.14	-0.76	3487.6
28	Eti-Oro	97	389	1911	370	2812	4.1	31.1	23.6	28.1	AKH	7.60	0.77	782.4
29	Iwaro	374	53	708	4026		2.0	7.4	32.3		HA	5.69	0.70	575.7
30	Iwaro	44	409	814	5417		5.3	10.3	21.8		AA	6.65	0.74	593.3
31	Akungba	98	193	495	7271		13.9	24.0	42.6		AA	14.69	0.87	336.4
32	Akungba	414	38	598	3256		1.7	4.9	45.7		HA	5.44	0.69	539.6
33	Akungba	145	57	651	6393		1.6	3.9	66.6		HA	9.82	0.82	607.6
34	Akungba	309	49	802	4282		1.6	4.7	68.8		HA	5.34	0.69	744.4
35	Akungba	263	75	693	3750		1.6	4.5	108.9		HA	5.41	0.69	662.8
36	Akungba	231	65	649	6941		3.0	7.2	74.1		HA	10.70	0.83	584.2
37	Ikare	524	86	4416	624	7744	6.4	18.5	38.5	23.9	HKH	12.41	0.85	2175.0
38	Ikare	397	61	36873	362	9708	22.2	24.5	28.5	34.0	HKH	26.82	0.93	9830.6
39	Ikare	220	159	2586	532	6987	9.7	38.6	28.1	33.4	HKH	13.13	0.86	899.0
40	Ikare	285	257	1055	273	4737	8.1	33.2	18.5	51.7	HKH	17.35	0.89	398.9
41	Ikare	96	209	1873	652	5615	6.3	37.6	24.0	35.7	AKH	8.61	0.79	740.3
42	Ikare	81	140	2121	505	5045	2.7	41.2	32.6	31.5	AKH	9.99	0.82	843.0

(a)   **A curve type**

(b)   **HK curve type**

(c)   **HA curve type**

(d) AA curve type

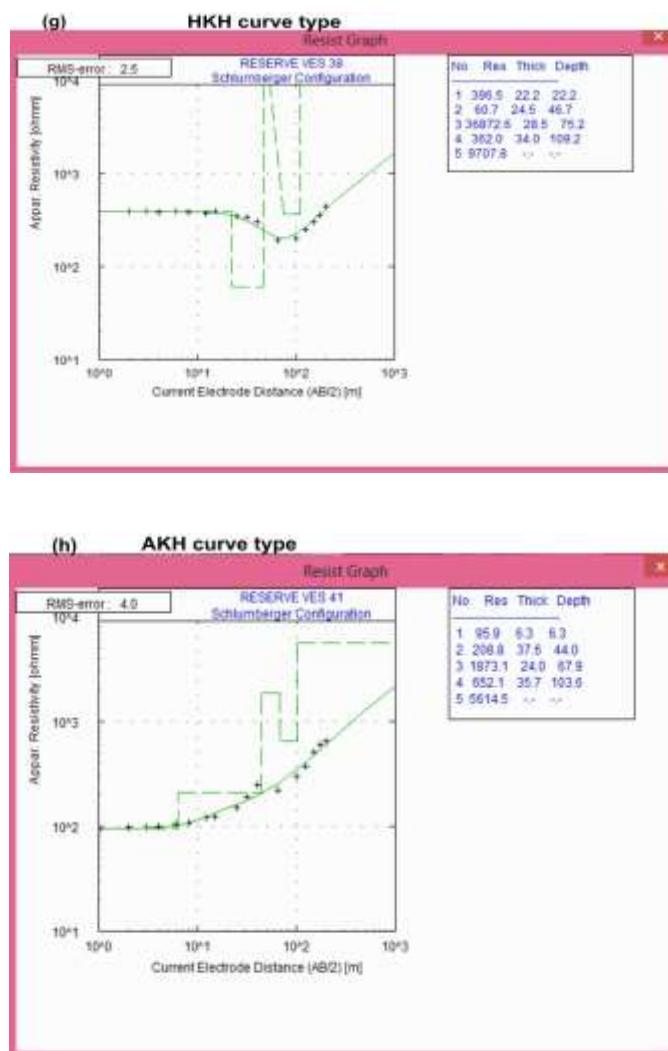(e) KH curve type

(f) KHK curve type

Figure 2: Distinctive curve types obtained from the geoelectric data of the area: (a) A curve type; (b) HK curve type; (c) HA curve type; (d) AA curve type; (e) KH curve type; (f) KHK curve type; (g) HKH curve type; (h) AKH curve type.
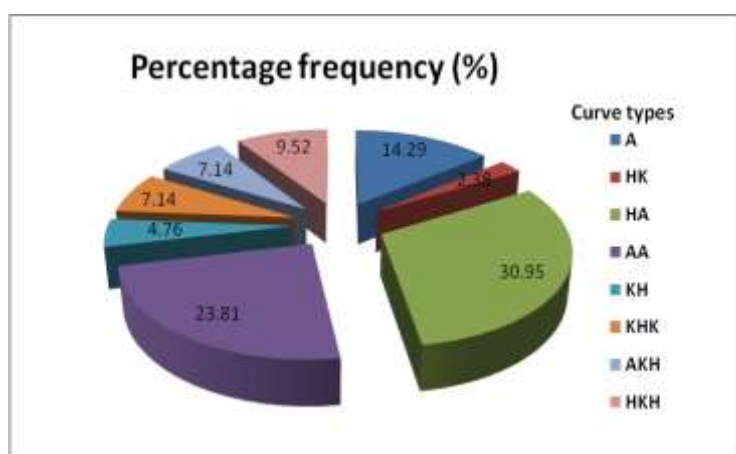

Figure 3: Percentage frequency of curve types acquired in the study area.

Subsurface geoelectrical characterization of the area

Geoelectric section across VES 7, 13, 19, 25 and 31

The geoelectric section across VES 7, 13, 19, 25 and 31 (Fig. 4) exhibits three to five subsurface layers. The resistivity of the top layer ranges from 77 – 426 Ωm and layer thickness within the range 1.6 – 20.2 m signifying clay, sandy clay and clayey sand lithology. There exist lateritic sandy layer beneath the top layer with respective resistivity and thickness in the range 437 – 1615 Ωm and 12.0 – 31.5 m at VES locations 13 and 25. The locations are also characterized by weathered bedrock with resistivity and thickness range of 82 – 193 Ωm and 5.6 – 24.0 m respectively. This clayey weathered profile is an indication of influence of intense weathering on the lithology. The existence of thick partially weathered/fractured rock layer (14. 4 m - ∞) with resistivity values in the range 351 – 836 (Fig. 4)

also revealed that the basement rock is structurally influenced by tectonic activities which enhance different geological structures on the rock deposit. This would also facilitate the exploitation of the rock deposits in the area. The resistivity of the fresh bedrock (1007 – 7271) with sufficient thickness in the range 26.9 – infinity (∞) would sustain a large scale exploitation scheme.
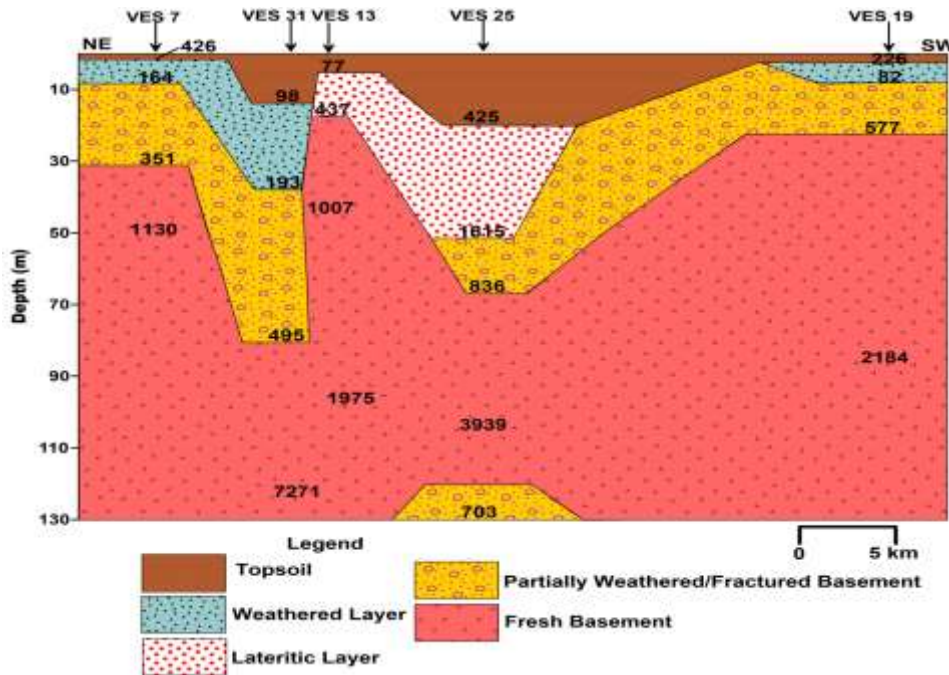

Figure 4: Geoelectric section from VES 7, 13, 19, 25 and 31 along NE-SW direction.

Geoelectric section across VES 3, 8, 14, 15 and 21
Three to five geologic layers are observed across the locations of VES 3, 8, 14, 15 and 21 (Fig. 5). Resistivity of the topmost layer of these locations (34 – 215 Ωm) with thickness range 3.4 - 10.8 m corresponds to clay and sandy clay. The locations are characterized with weathered rock layer (73 – 144 Ωm) of clayey facies beneath VES 8 and 15 with thickness range of 7.7– 13.7 m (Fig. 5). The topmost layer is underlain by laterite at locations VES 3, 14 and 21 with resistivity and thickness range of 369 – 430 Ωm and 5.3 – 17.4 m respectively. The partially weathered/fractured rock layer has resistivity range of 503 - 663 Ωm with thickness 22.8 – 26.9 m (Fig. 5), while the resistivity of the massive fresh bedrock varies from 1372 – 7036 Ωm which is considered economically viable for sustainable mining.
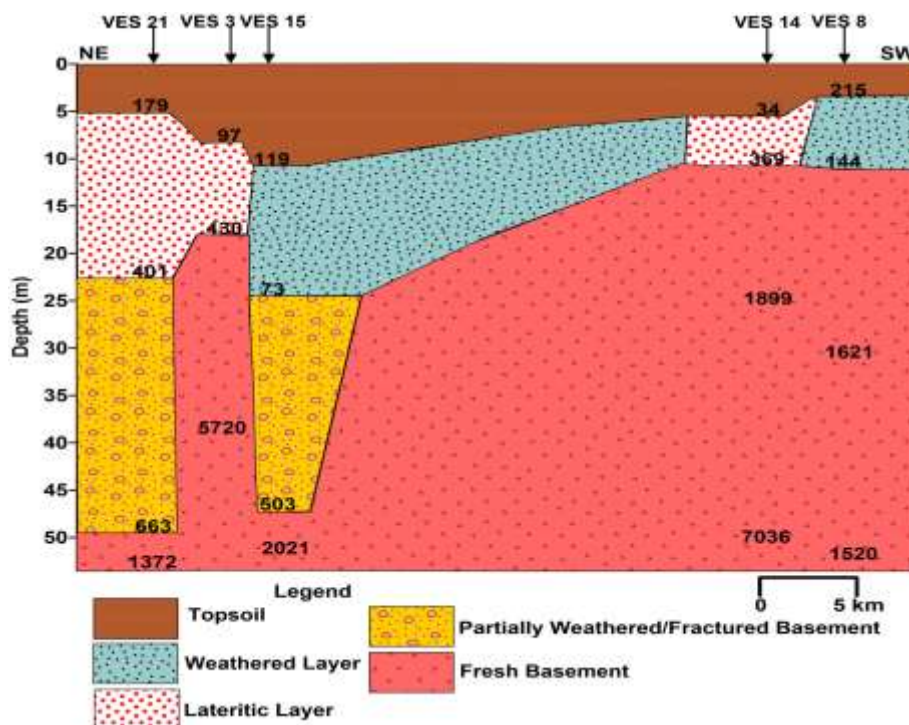

Figure 5: Geoelectric section from VES 3, 8, 14, 15 and 21 along NE-SW direction.

Geoelectric section across VES 20, 26, 32, 37 and 38
The locations beneath VES 20, 26, 32, 37 and 38 shows four to five geologic units. The topsoil of these locations is dominated by sandy clay/clayey sand/laterite with resistivity range of 210 – 524 Ωm and thickness 1.7 – 22.2 m (Fig. 6). Weathered rock layer cut across all the locations except VES 26, having resistivity (38 – 86 Ωm) indicating clay composition as a result of influence of weathering on the rock of the area. Partially weathered /fractured rock layer beneath all the locations with resistivity range 362 – 884 Ωm are extensively thick (23.9 m – infinity) capable of supporting large scale mining in the area. This thickness guarantees sustainable exploitation of the migmatite-gneiss deposit for industrial and economical purposes. The bedrock topography is irregular with resistivity of the massive fresh bedrock ranging 1926– 36873 Ωm (Fig. 6).
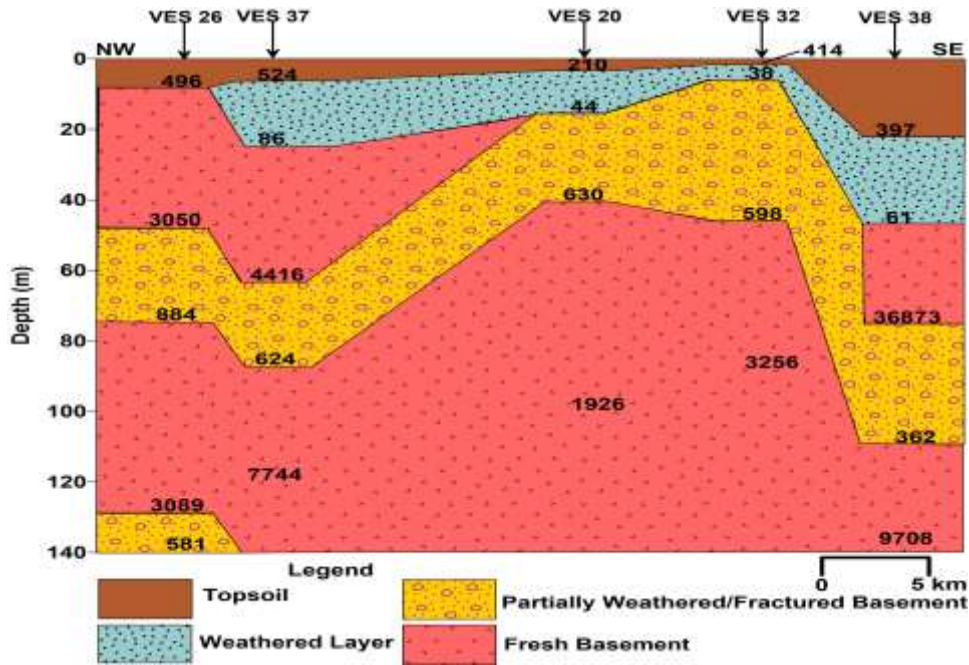
Figure 6: Geoelectric section from VES 20, 26, 32, 37 and 38 along NW-SE direction.

Geoelectric section across VES stations 1, 4, 9, 27, 33 and 39
The subsurface section of these locations of VES 1, 4, 9, 27, 33 and 39 (Fig. 7) is characterized by three to five different geologic layers with depth. Sandy clay dominates the topsoil with laterite in some places. Relatively resistive formation characterized the topsoil (100 – 451 Ωm) of thick, 1.6 – 19.7 m sandy clay and clayey sand. The weathered rock layer possesses resistivity between 57 and 159 Ωm and 3.9 – 38.6 m thickness. The topsoil is underlain by thick layer of lateritic formation (6.9 and 8.0 m) with 466 and 497 Ωm resistivity response beneath VES stations 1 and 4. Partially weathered/fractured rock layer (532 – 848 Ωm) having thickness range 17.5 m – infinity (∞) is localized at VES locations 27, 33 and 39. The fresh bedrock has resistivity range 1106 – 6987 Ωm with depth to basement 10.5 – 109.8 m. High thickness of these rock layers would encourage its mining for economic purposes.
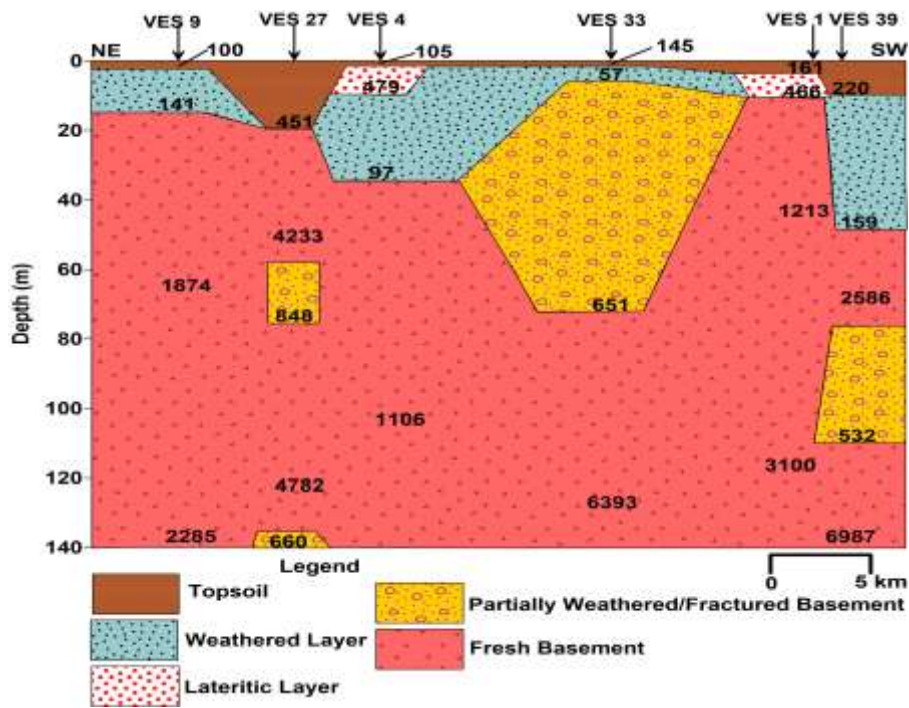
Figure 7: Geoelectric section across VES stations 1, 4, 9, 27, 33 and 39 along NE-SW direction.

Geoelectric section across VES stations 2, 5, 10, 16, 22, 28, 34 and 40

The geologic section of these locations reveals three to five different subsurface rock layers (Fig. 8). Topsoil resistivity and thickness range of these locations; 41 – 309 Ωm and 1.4 – 12.6 m corresponds to clay and sandy clay of the layer. The weathered geologic unit composed of clay (48 and 49 Ωm) majorly exists beneath VES 10 and 34 with thickness 6.7 and 4.7 m respectively. All the locations except VES 10 and 34 are characterized by lateritic formation of resistivity and thickness range of 257 – 666 Ωm and 14.2 – 33.2 m. The partially weathered/fractured rock unit possesses resistivity and thickness in the range 273 – 802 Ohm-m and 16.0 – 68.8 m respectively, cross-cut all the locations except VES stations 2, 5 and 16 (Fig. 8). The thickness of this geologic rock unit indicates that the fractured rock layer form a viable location/site for mining with maximum rock aggregates productivity in building, construction and extractive industries. The fresh bedrock at these locations is characterized by resistivity range 1025 – 4737 Ωm (Fig. 8).
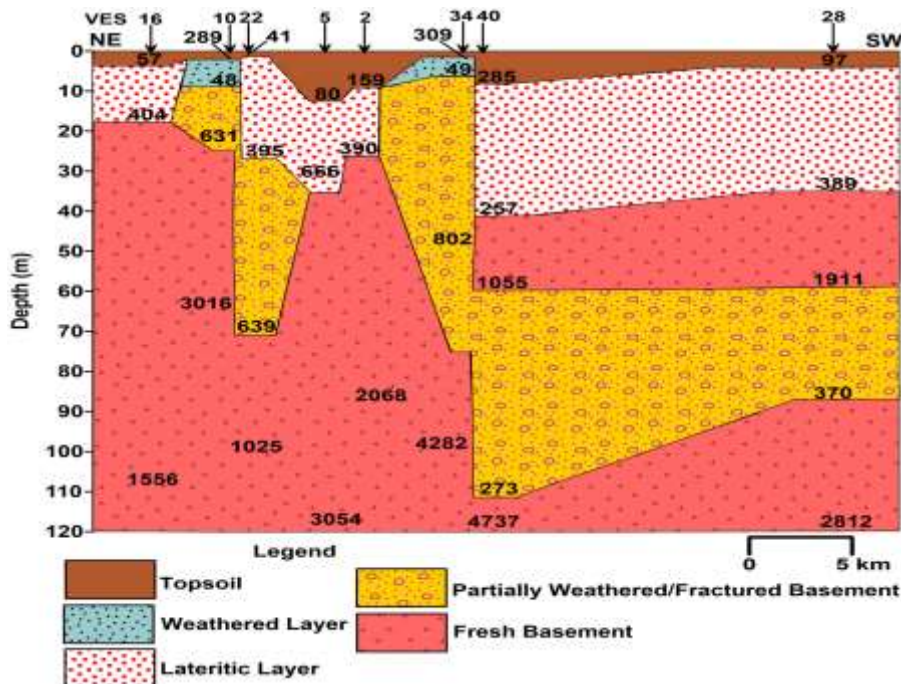

Figure 8: Geoelectric section across VES stations 2, 5, 10, 16, 22, 28, 34 and 40 along NE-SW direction.

Geoelectric section across VES stations 6, 11, 17, 18, 23, 29, 35 and 41

Three to five geologic rock units are established across VES stations 6, 11, 17, 18, 23, 29, 35 and 41 (Fig. 9). The resistivity range of 59 – 490 Ωm dominated the topsoil signifies clay/sandy clay/clayey sand/lateritic clay having thickness varying from 1.1 – 6.8 m. The weathered rock unit of resistivity < 210 Ωm implies clayey and sandy clay composition with relative thickness of 4.0 – 37.6 m. Deep weathering of rock unit observed at VES station 41 to the depth of 44.0 m suggests that the rock at this zone is subjected to intense influence of weathering on the rock type with resultant sandy clay formation. Different structural geological features (fracture, fault, lineament, lithological contacts, and unconformity) observed on some of the rock outcrops are indication of tectonic activities of the terrain. The fractured rock unit cut across all the locations with resistivity variations of 553 – 865 Ωm with thickness range of 11.1 – 108.9 m. The locations are characterized by uneven bedrock topography with fresh bedrock resistivity range 1670 – 5615 Ωm. Considering the resistivity and thickness of the rock layers, they are viable sites for optimum aggregate productivity and sustainability to enhance large scale mining development in the area.
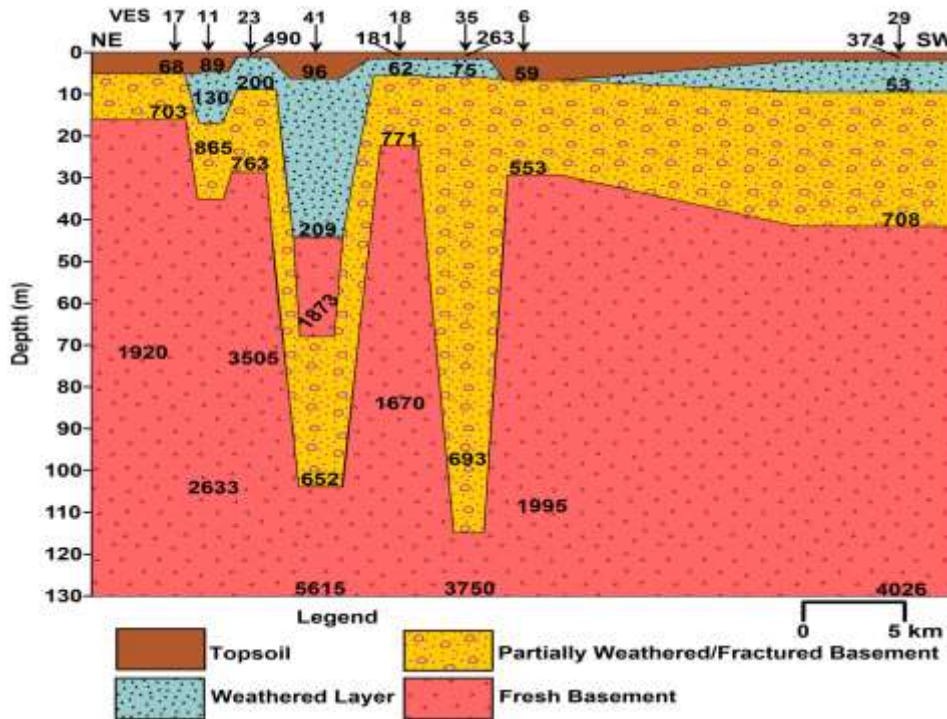

Figure 9: Geoelectric section across VES stations 6, 11, 17, 18, 23, 29, 35 and 41 along NE-SW direction.

Geoelectric section across VES stations 12, 24, 30, 36 and 42

Four to five lithologic units are observed across VES stations 12, 24, 30, 36 and 42 (Fig. 10). The resistivity range of the topsoil from 44 – 413 Ωm indicates clay/sandy clay and clayey sand with thickness range of 2.7 – 9.5 m. The weathered bedrock of these locations with resistivity varying from 65 – 209 Ωm and thickness 7.2 – 41.2 m localized at VES stations 12, 36 and 42 signifies clay and sandy clay. The depth of 43.9 m exhibited by weathered bedrock at VES station 42 suggests deep weathering of the rock at this location resulting to its clayey formation. The occurrence of lateritic sand (409 – 1197 Ωm) beneath the topsoil at VES 24 and 30 constitutes the lateritic layer having thickness range of 10.3 – 28.5 m (Fig. 10). The partially weathered/fractured bedrock (505 - 944 Ωm) transverses all the locations have thickness varying from 18.4 – 74.1 m. The great depth of the rock unit (37.5 – 107.9 m) would facilitate and sustain large scale mining of the migmatite gneiss deposit for economic purposes. Resistivity variation of the fresh bedrock (1353 – 6941 Ωm) as revealed by the subsurface geologic image signifies irregular basement topography of the area.
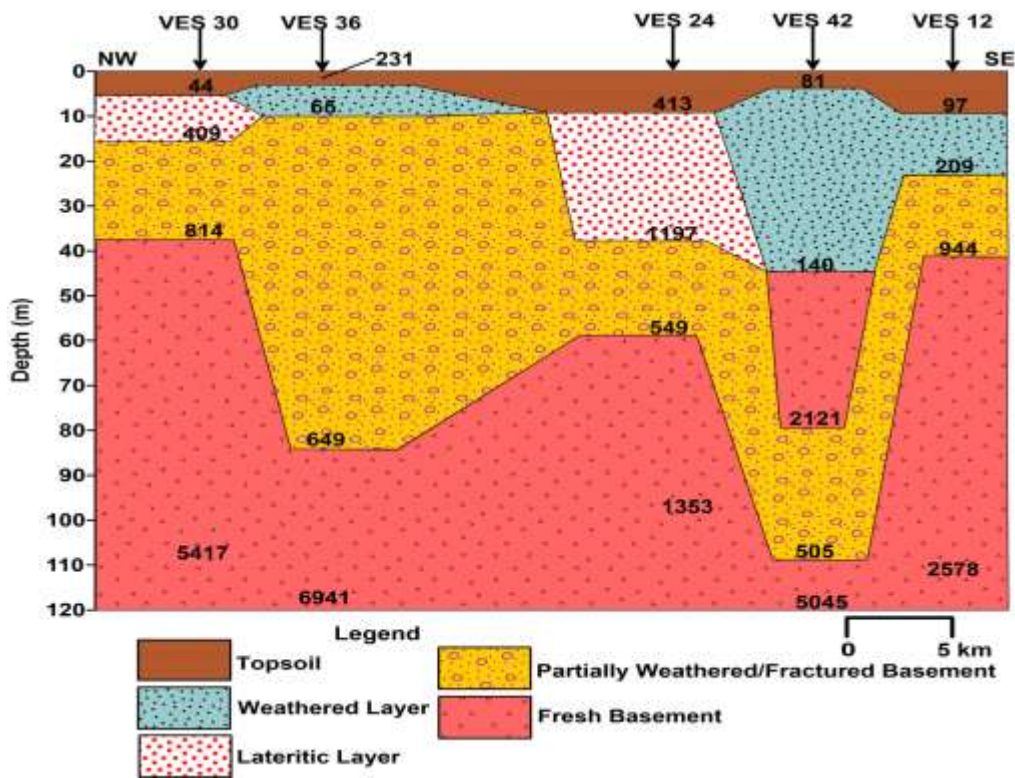
Figure 10: Geoelectric section across VES stations 12, 24, 30, 36 and 42 along NW-SE direction.

Bedrock/Basement characterization

The resistivity of the fresh bedrock in the study area ranges from 1007 - 36873 Ωm (Table 2) with mean resistivity 4303 Ωm indicates freshness of the geological basement terrain devoid of weathering. Geologically, irregular bedrock weathering constitutes variability in the resistivity of the bedrock with resultant uneven basement topography (Fig. 11a). The basement topography map (Fig. 11b) reveals the geomorphology of the area, which could assist in predicting suitable sites for rock prospect. High topographical zones (basement ridges) in the northeastern, northwestern and southeastern parts (Fig. 11b) serve as best zones viable for mining. Fracture occurrence within the bedrock

observed across the area with resistivity between 273 and 944 Ωm forms the fractured basement. This is indicated as high fractured basement rock in the area with resistivity > 750 Ωm indicating low influence of weathering on the basement rock. Resistivity zones of above 3000 Ωm observed in the northwestern, northeastern and some portions of the southwestern parts of the area (Fig. 12) indicate fresh bedrock/basement devoid of weathering. The high resistive regions confirm the freshness of the basement topographical highs at the northeastern, northwestern and southeastern parts of the area. These regions are considered appropriate for exploitation of substantial civil engineering construction rock aggregates.
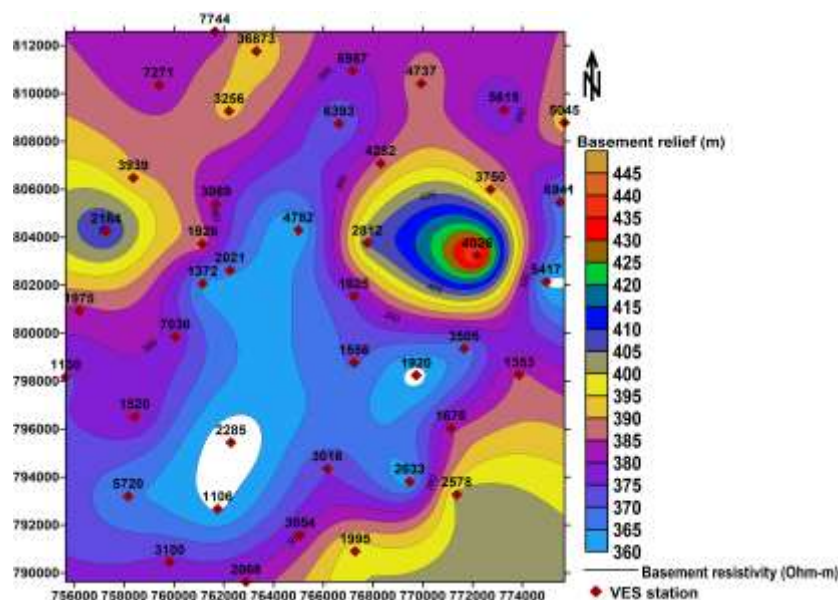

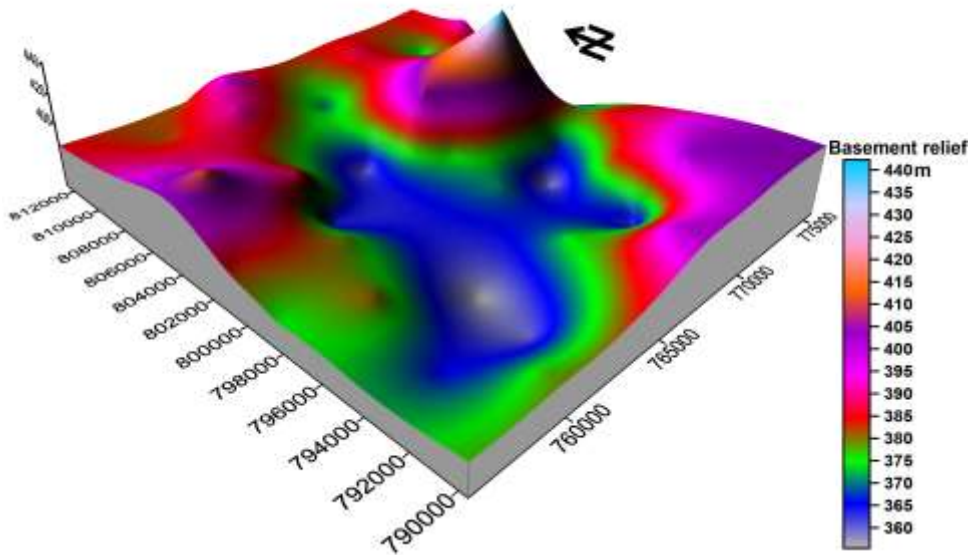**Figure 11a:** Basement topographical view of the area.

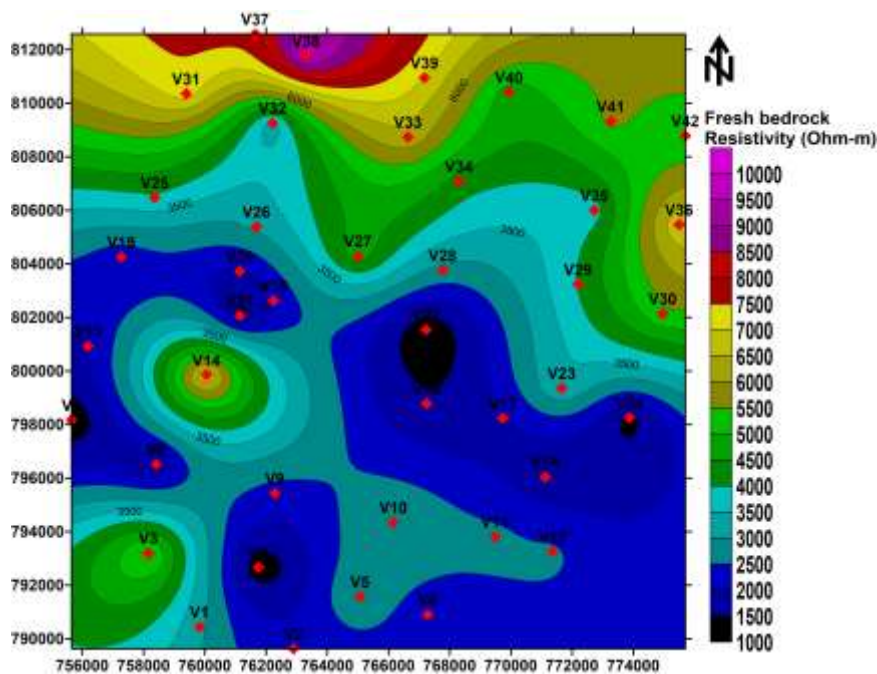**Figure 11b:** 3D basement view of the area.

Figure 12: Basement resistivity view of the area.

Resistivity contrast and reflection coefficient

The resistivity contrast and reflection coefficient (R_c) are projected geoelectrical parameters used to evaluate the extent of weathering of the basement and its freshness (Olayinka, 1996). The basement is characterized by resistivity contrast 0.14 – 26.82 with mean 6.02±5.39 (Fig. 13) and geoelectrical reflection coefficient in the range -0.76 – 0.93 (Fig. 14) with average 0.52±0.41. High resistive fresh basement of the northeastern, northwestern and southeastern parts reveals resistivity contrast above 14 and reflection coefficient ≥ 0.7 (Figs 13 and 14). The basement resistivity, resistivity contrast and reflection coefficient confirm the freshness of the northeastern, northwestern and southeastern dominated basement. The underlain fresh basement of the northeastern, northwestern and southeastern regions is significant for maximum and sustainable mining exploitation in the area.
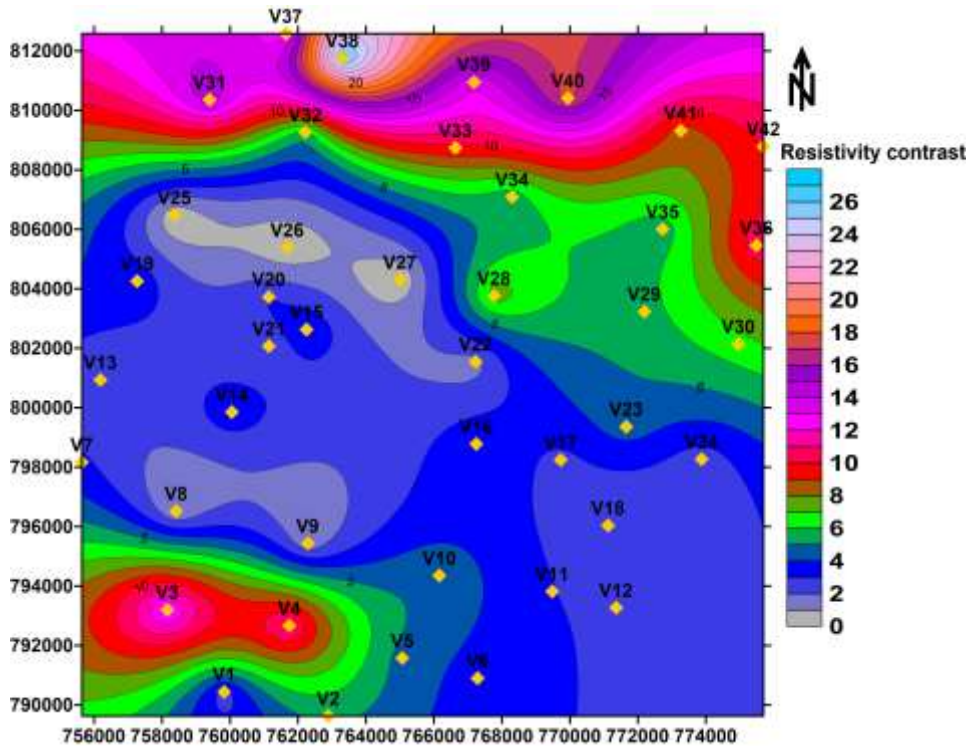
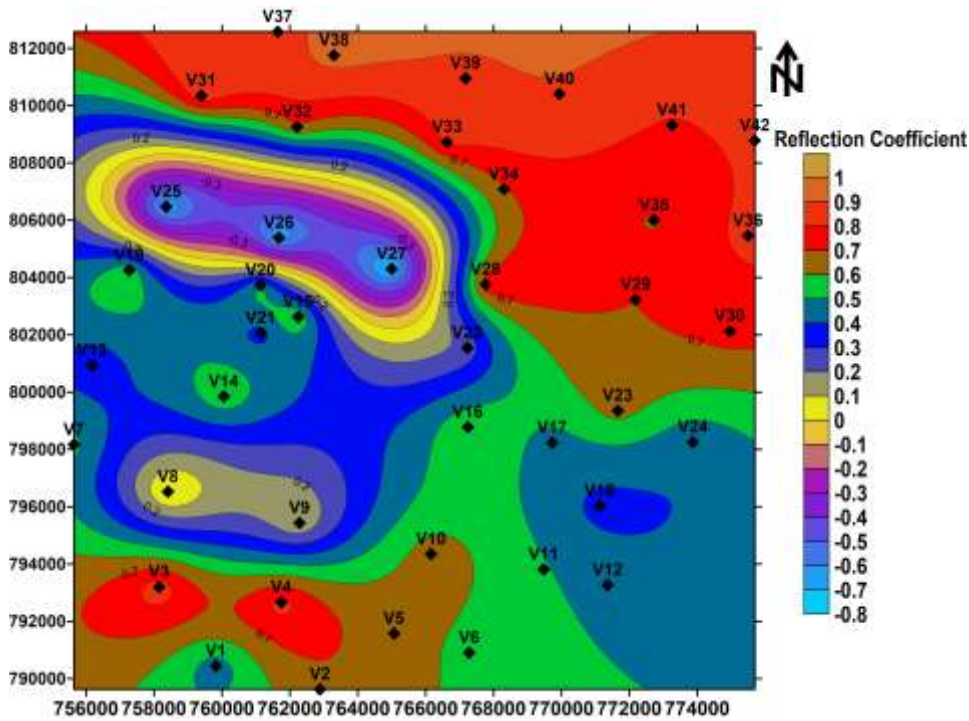**Figure 13:** Resistivity contrast view of the migmatite-gneiss deposit.

Figure 14: Reflection coefficient map of the migmatite-gneiss deposit.

Transverse layer resistivity (ρ$_T$) and Reserve estimation of the migmatite gneiss

Transverse layer resistivity (ρ$_T$) is one of the Dar-Zarrouk parameters for a single geologic layer or sum total of multiple geologic rock units, estimated from the subsurface modeled parameters (Singh, 2005) to establish the quality of the migmatite-gneiss deposits in the area. The ρ$_T$ of the deposits varies from 185.7 – 9831.0 Ωm (Table 2 and Fig. 15) with mean 1005.0 ± 1545.1 Ωm, classifies worth of the deposits for different purposes. Higher ρ$_T$ (> 500 Ωm) experience across the

area signifies good quality fresh deposits than other regions particularly the southwestern part of ρ$_T$ less than 500 Ωm (Fig. 15). Thus, good quality fresh migmatite-gneiss deposits of the study area show its high prospects for sustainable mining development. The thickness of the migmatite-gneiss deposits ranges 8.0 – 108.9 m (Fig. 16) to infinity (∞) with average thickness of 29.3 m and thicker deposit at the northeastern and northwestern parts of the area. With the observed quality of the deposit, this study reveals that the migmatite gneiss deposit is thicker where the deposit is

fresh and less weathered. The average thickness of the migmatite-gneiss deposits (29.3 m) acquired across the area was used to quantify the deposits.

The volume of the migmatite gneiss deposit is calculated as the average deposit thickness (29.3 m) multiply by the area extent…………...(1)

Where the average deposit thickness was estimated from the addition of the thicknesses of the migmatite gneiss deposits, divided by total number of VES stations occupied.

=1230.3/42

= 29.2929 m ≈ 29.3 m

The area extent of the locations of the study area was estimated from ground mapping measurement as 71,300,000 m^2.

Thus, volume of the migmatite gneiss deposit = 29.3 m × 71,300,000 m^2

= 2,089,090,000 m^3

The reserve tonnage of the migmatite gneiss deposit is estimated using the equation:

Migmatite gneiss reserve estimate = estimated volume of the migmatite gneiss deposit × average migmatite gneiss rock density (2700 kg/m^3)………………………………….. (2)

= 2,089,090,000 m^3 × 2700 kg/m^3

= 5,640,543,000,000 kg (mass/weight of the migmatite gneiss deposits)

Reserve estimate of the migmatite-gneiss deposits in tonnes = 5,640,543,000,000/1000

= 5,640,543,000 tonnes.

The variogram plotted (Fig. 17) shows the variability and spatial correlation between the acquired data with respect to its location. The result of the statistical analysis illustrated in Table 3 shows a relatively low coefficient of variation of the data with positive skewness and kurtosis. The positive skewness and kurtosis exhibited by the data (Table 3) reveals asymmetric, uneven and peaked data distribution relative to statistical data distribution. The relatively low nugget value signifies no particular pattern of the data, thus, any suitable exploration pattern is suggested. The area extent and volume of the migmatite-gneiss deposits were respectively estimated as 71,300,000 m^2 and 2,089,090,000 m^3. The distantly-spaced data points and sill (corresponds to statistical variance; where the graph flattens out) of the variogram (Fig. 17) reveals degree of variability with positive correlation signifying connection of the estimated variance from the variogram data points and the location. Thus, the reserve estimate of the migmatite gneiss deposits of the study area is 5,640,543,000 tonnes. This signifies substantial deposit for sustainable large scale mining of the migmatite gneiss as construction rock aggregates and other applications for economic purposes.

Table 3: Statistical analysis of the thickness of the migmatite gneiss deposits

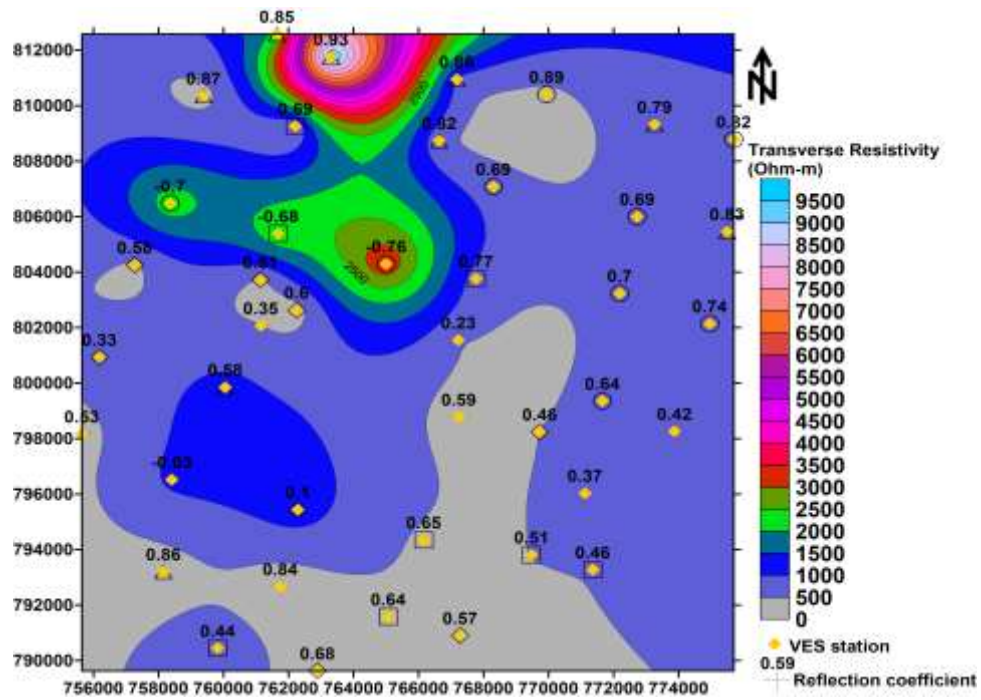| Statistical parameters	Migmatite-gneiss thickness
Range (m)	100.90
Sill	388.26
Standard deviation	19.70
Coefficient of variation	0.67
Coefficient of skewness	2.10
Kurtosis	5.67
Reserve estimate of the migmatite-gneiss deposits	
Area extent (m^2)	71,300,000
Total volume (m^3)	2,089,090,000
Mass (kg)	5,640,543,000,000 kg
Reserves tonnage	5,640,543,000 tonnes

Figure 15: Transverse resistivity view of the migmatite-gneiss deposit.
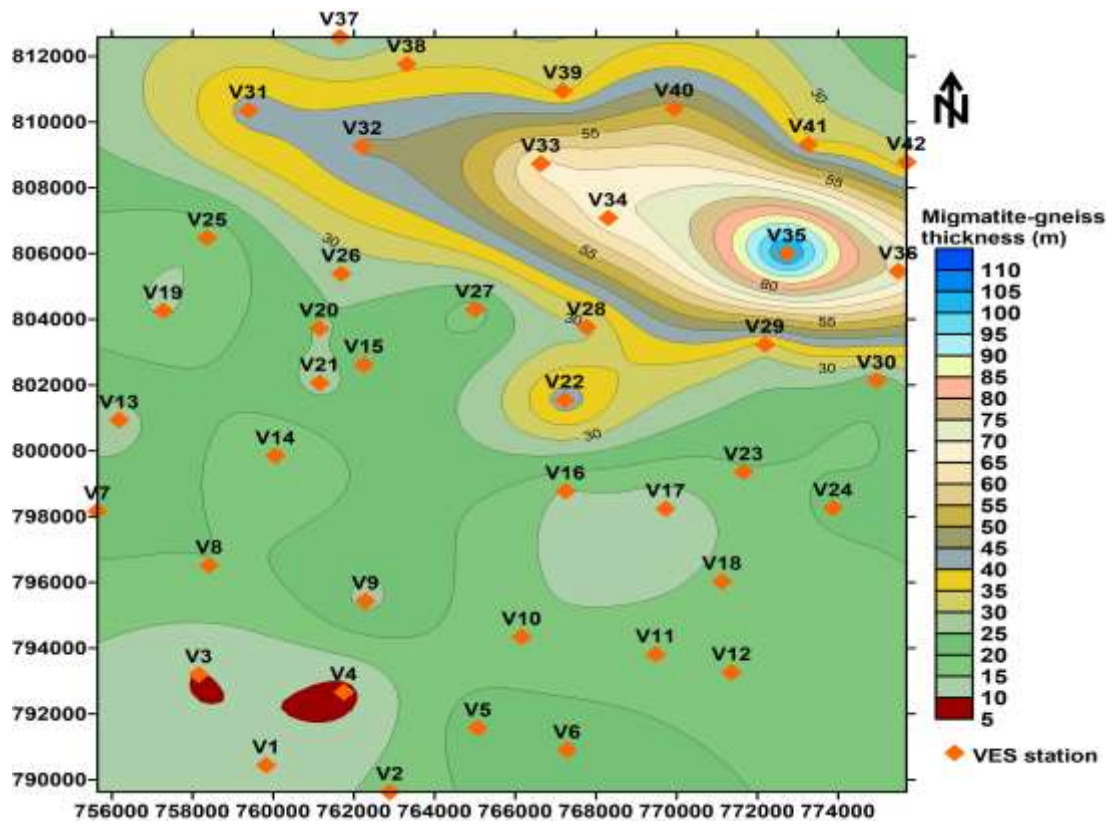

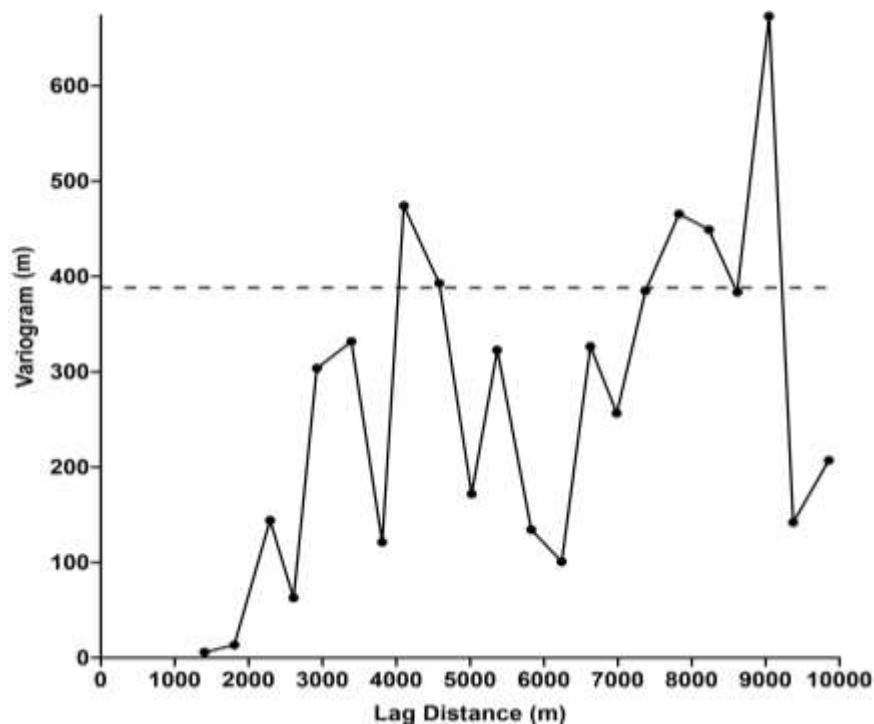**Figure 16:** Thickness distribution of the migmatite-gneiss deposit.

Figure 17: Variogram plot of the migmatite-gneiss deposit thickness of the area.

CONCLUSION

Migmatite gneiss has increasingly been acknowledged as construction aggregate due to its strength and other unique features. The quantity of migmatite-gneiss deposits in parts of southwestern Nigeria was assessed and estimated for construction aggregates and other applications. Comprehensive geological field mapping, geoelectrical resistivity and laboratory density measurements were employed for the resource quantification. The extent of migmatite gneiss and its contacts with other rocks were mapped and led to the production of detailed geological map of the area. The electrical resistivity investigation employed Schlumberger vertical electrical sounding (VES) technique with a total of forty-two sounding stations across the entire area of study. The processed data offer the resistivity and thickness of different layers of subsurface geomaterials at every VES station. Seventeen (17) fresh rock samples were collected from different migmatite-gneiss rock outcrops across the study area were taken to the laboratory for density measurement from which the mean density of the migmatite-gneiss deposits was determined. Geostatistical analysis was used to estimate the spatial correlations of the data acquired to predict accuracy of the values based on relationship between location and acquired data. The results were analyzed to establish the density and thickness of the deposits. The density range of migmatite-gneiss in the study area is 2.56 – 2.88 g/cm^3 with an average density of 2.70 ± 0.10 g/cm^3. Subsurface information and disposition of different locations investigated is revealed by resistivity responses of geomaterials of the area. Eight different VES curve types (A, AA, HA, HK, KH, AKH, HKH and KHK) are obtained from the processed geoelectric field data with predominant HA curve type (31% occurrence) followed by AA (24%), A (14%), HKH (10%), AKH, KHK (7%), KH (5%) and HK (2%). High occurrence of HA followed by AA type curves signify complex geologic

setting of the area with high resistive bedrock (host rock). The curve types show that three to five distinctive subsurface layers characterized the geologic sequence existing in the area. The subsurface geologic layers include top layer (topsoil), weathered rock layer, lateritic layer, partially weathered/fractured rock layer and fresh basement. Thick fractured rock layer localized in the area would facilitate the exploitation of the migmatite-gneiss deposits as construction aggregates for sustainable socio-economic development of the area and its environs. High topographical zones (basement ridges) at the northeastern, northwestern and southeastern parts also serve as the best zones viable for mining. High resistivity range (> 3000 Ωm) of the basement topographical highs confirms its freshness. The basement resistivity, resistivity contrast and reflection coefficient corroborate the freshness of the northeastern, northwestern and southeastern dominated basement. Higher ρ_T (> 500 Ωm) across the area signifies good quality fresh migmatite-gneiss deposits of the area except the southwestern part with ρ_T less than 500 Ωm. Thus, good quality fresh migmatite-gneiss deposits of the study area show high prospects for sustainable mining development with average thickness of 29.3 m. The deposit is thicker at the northeastern and northwestern parts of the area where the deposit is fresh and less weathered. The area extent and estimated volume of the migmatite-gneiss deposits of the study area are 71,300,000 m^2 and 2,089,090,000 m^3 respectively. The distantly-spaced data points of the variogram reveal a high degree of variability with positive correlation signifying connection of the estimated variance and location of data points. The reserve estimate of the migmatite gneiss deposits of the study area is 5,640,543,000 tonnes. This signifies substantial deposits for sustainable large scale mining. The location, spatial orientation, size and shape of the migmatite-gneiss deposits of the area suggests a first step of open cast mining, upon which deeper sections of

the deposits could be exploited by underground mining technique. These findings would be beneficial to government and other entrepreneurs for investments.

REFERENCES

Ademila, O., 2019. Engineering Geological Evaluation of Some Rocks from Akure, Southwestern Nigeria as Aggregates for Concrete and Pavement Construction. Geology, Geophysics and Environment, 45(1): 31-43.

Ademila, O., 2019. Geotechnical properties and effects of palm kernel shell ash and cement on residual soils in pavement construction along Owo-Ikare Road, Southwestern Nigeria. The Pacific Journal of Science and Technology, 20(1): 365-381.

Ademila, O., 2021. Combined geophysical and geotechnical investigation of pavement failure for sustainable construction of Owo-Ikare highway, Southwestern Nigeria. National Research Institute of Astronomy and Geophysics (NRIAG) Journal of Astronomy and Geophysics, 10(1): 183-201.

Ademila, O., 2022. Pre-foundation geophysical investigation of a site for structural development in Oka, Nigeria. National Research Institute of Astronomy and Geophysics (NRIAG) Journal of Astronomy and Geophysics, 11(1): 81-112.

Ademila, O., Olayinka, A. I. and Oladunjoye, M. A., 2020. Land satellite imagery and integrated geophysical investigations of highway pavement instability in Southwestern Nigeria. Geology, Geophysics and Environment, 46(2): 135-157.

Bufford, K. M., Atekwana, E. A. and Abdelsalam, M. G., 2012. Geometry and faults tectonic activity of the Okavango rift zone, Botswana: evidence from magnetotelluric and electrical resistivity tomography imaging. Journal of African Earth Sciences, 65: 61-71.

Hamblin, W. K. and Howard, J. D., 2005. Exercise in Physical Geology, Pearson Education Inc., Upper Saddle River, NJ, 297pp.

Heriawan, M. N. and Koike, K., 2008. Uncertainty assessment of coal tonnage by spatial modeling of seam distribution and coal quality. International Journal of Coal Geology, 76: 217-226.

Koefoed, O., 1979. Geosounding principles 1; Resistivity sounding measurements. Elsevier Scientific Publishing Company, Amsterdam, 275pp.

Kokesz Z., 2006. Application of linear geostatistics to evaluation of Polish mineral deposits, Gospodarka Surowcami Mineralnymi, Tom 22 2006, Zeszyt, 2: 53-65.

Marshak, S., 2013. Essentials of Geology (4th edition). W.W. Norton, pp. 194-195. ISBN 979-0-393-91939-4.

Olayinka, A. I., 1996. Non-uniqueness in the interpretation of bedrock resistivity from sounding curves and its hydrogeological implications. Water Resources Journal of the Nigerian Association of Hydrogeologists, 7(1 and 2): 49-56.

Pawley, M. J., Reid, A. J., Dutch, R .A. and Preiss, W. V., 2015. Demystifying migmatites: an introduction for the field-based geologist; Applied Earth Science (Transactions of the Institutions of Mining and Metallurgy, Section B), 124(3): 147-174. DOI: 10.1179/1743275815Y.0000000014.

Rahaman, M. A., 1989. Review of the basement geology of Southwestern Nigeria. In: Kogbe C.A. (Editor). Geology of Nigeria (2nd ed.), Rock View Nigeria Limited, Jos. 39-56.

Rahaman, M. A. and Ocan, O., 1978. On the relationship in the Precambrian migmatite-gneiss of Nigeria. Journal of Mining and Geology, 15(1): 23 -32.

Robertson, S., 1999. British Geological Survey rock classification scheme, Volume 2 - Classification of metamorphic rocks; British Geological Survey Research Report, RR 99-02, 28pp.

Sawyer, E. W., 2008. Atlas of migmatites. The Canadian Mineralogist Special Publication 9, NRC Research Press, Ottawa, Ontario, Canada, 371pp.

Singh, K. P., 2005. Nonlinear estimation of aquifer parameters from surficial resistivity measurements. Hydrology and Earth System Sciences Discussion, 2: 917-938.

Telford, W. M., Geldart, L. P., Sheriff, R. E. and Keys, D. A., 1990. Applied Geophysics. 2nd ed. Cambridge: Cambridge University Press, pp.344–536.

Vander Velper, B. P. A., 2004. WinResist version 1.0 resistivity depth sounding interpretation software. ITC (Delft Netherland): M.Sc. Research Project.

Ward, S. H., 1990. Resistivity and induced polarization methods. In Geotechnical and Environmental Geophysics, Vol. 1, ed. S.H. Ward, Tulsa, OK: Society of Exploration Geophysicists, pp. 147–190.

Zohdy, A. A. R., 1973. A computer program for automatic interpretation of Schlumberger sounding curves over horizontally stratified media. PB-232703, National Technical Information Service, Springfield, Virginia, 25 pp.